

# Study of sodium depositions in heart interstitium using methods of X-ray absorption and X-ray fluorescence microscopy

Igor A. Artyukov<sup>\*a</sup>, Grigori P. Arutyunov<sup>b</sup>, Maksim A. Bobrov<sup>c</sup>, Inna N. Bukreeva<sup>a,d</sup>, Alessia Cedola<sup>d</sup>, Dmitri O. Dragunov<sup>b</sup>, Ruslan F. Feshchenko<sup>a</sup>, Michela Fratini<sup>d</sup>, Alessandra Gianoncelli<sup>e</sup>, Vadim M. Mitrokhin<sup>b</sup>, Anna V. Sokolova<sup>b</sup>, Alexander V. Vinogradov<sup>a</sup>

<sup>a</sup>P.N.Lebedev Physical Institute RAS, 53 Leninsky Prospekt, Moscow, Russia 119991;

<sup>b</sup>Pirogov Russian National Res. Medical University, 1 Ostrovitianov St., Moscow, Russia 117997;

<sup>c</sup>Moscow Regional Research and Clinical Institute, 61/2 Shchepkina St., Moscow, Russia 129110;

<sup>d</sup>CNR-Institute of Nanotechnology, 5 Piazzale Aldo Moro, Rome, Italy 00185;

<sup>e</sup>ELETTRA-Sincrotrone Trieste, S.S. 14, km 163.5 in Area Sci. Park, Basovizza-Trieste, Italy 34149

## ABSTRACT

To date there have been only indirect indications of the presence of bound sodium accumulation in muscle and skin tissues. Despite their osmotic inactivity, such sodium deposits can effect on mechanical properties of the heart muscle impairing its elasticity and leading to serious heart dysfunctions. In this work an accurate study of the chemical composition of the heart muscle tissue at the cellular level was carried out using the methods of X-ray absorption and fluorescence microscopy. The experiments were carried out on a TwinMic X-ray scanning microscope [3] at ELETTRA synchrotron (Italy) with a resolution of about 1  $\mu\text{m}$ . Comparison of the obtained maps of intra- and extracellular sodium distribution in heart tissues of different laboratory animals has resulted in the first experimental confirmation of the hypotheses about the existence of deposited sodium states in the intercellular space. The paper demonstrates an example of the state-of-the-art medical applications of high spectral brilliance X-ray sources.

**Keywords:** X-ray microscopy, X-ray fluorescence microanalysis, XRF, SXR, myocardia, sodium deposits

## 1. INTRODUCTION

The sodium-related homeostasis processes are an important part of the vital functions of an organism. Sodium intake, retention and excretion are naturally regulated to balance between the salt and water content with a high accuracy of 1-2%. Any sodium concentration misbalances are known to cause serious diseases and malfunction of the body including a loss of myocardia function<sup>1</sup>. Recent studies indicate that homeostasis of sodium is much more complex than previously thought; it includes not only kidneys but also skin and muscle tissues<sup>2-4</sup>.

At the end of the 20<sup>th</sup> century, a previously unknown type of “passive” sodium was suggested to exist following the fact that negatively charged glycosaminoglycans (GAGs) of the extracellular matrix may bind to positively charged cations of light metals. Thus, a part of sodium content becomes osmotically neutral enough to leave the active homeostasis process and to stop its influence on the values of arterial pressure (AP) and extracellular fluid volume<sup>3</sup>. However, the sodium deposits continue to affect the properties of adjacent tissues. Thus, an excessive concentration of sodium in GAG can initiate new biological processes involving the macrophages<sup>4</sup>.

In 2007-2012 the prolonged and accurate study of bodily sodium intake/excretion ratio<sup>5</sup> discovered the amounts of excreted sodium not related directly to the sodium intake and arterial pressure values. This fact was explained by the existence of osmotically passive sodium deposits in skin and muscle tissues formed earlier that can deplete to contribute to the elevated level of sodium in urine. To visualize these sodium accumulations M. Hammon et al. used <sup>23</sup>Na Magnetic Resonance Imaging (MRI) of the lower legs<sup>6</sup> and M Christa et al. observed an increased sodium MRI signal in

---

\* iart@lebedev.ru; phone 7 499 132-6522; fax 7 499 135- 7880; www.lebedev.ru

myocardia<sup>7</sup>. However, low spatial resolution and weak intensity of sodium MRI signal did not allow studying the sodium concentration peaks at the cell scale.

Several years ago our group carried out a series of acoustical and X-ray fluorescence analysis (BRUKER S8 Tiger spectrometer) investigations of chemical and mechanical properties of the heart tissues of 18 deceased patients<sup>8</sup>. We found a correlation between elevated sodium concentration in heart muscles, patient's age and arterial hypertension. Also there was evidence of sodium-related modification of muscle elasticity of myocardia and related diastolic function. However, these experiments also lacked high spatial resolution needed for studying the sodium localization at the cell level.

This paper presents the results of X-ray fluorescent and absorption microscopy experiments based on high brilliance X-ray source on detection and analysis of sodium depositions in the extracellular matrix of myocardial tissues of rats with the reference to their sodium intakes.

## 2. THE SAMPLE PREPARATION

The samples of heart tissues were taken from different laboratory animals\*. Two groups of 15 Wistar rats aged 15-16 weeks were grown, with the sodium consumption rate of these two groups being different from the third week. The low sodium diet limited the sodium intake by the value of 0.2 mEq per 200 g of body weight per day, while the high sodium diet ration contained 2.0 mEq or more per 200 g of body weight per day. In other words, two groups were distinguished by sodium intake rates as normal (control group) and extensive<sup>9,10</sup>. The water supply was always kept as ad libitum (25 ml of de-ionized water for 15 g of food) and the food ration was about 15 g per 200 g body weight per week for all the animals.

High sodium diet feeding was maintained in the corresponding group of animals during 8 weeks before the myocardial hypertrophy occurred<sup>11</sup>. After 8 weeks the animals were intraperitoneally injected with methohexital at a dose of 100 mg/kg and sacrificed through decapitation.

The 3- $\mu$ m thick slices of the paraffin-fixed myocardia were cut from the extracted heart tissues, then mounted onto slides and dried ( $T = 60^\circ\text{C}$ ) in the air. Finally, paraffin was removed with ethanol and the slices were stained by hematoxylin and eosine in accordance with standard histological procedures. For X-ray studies, the slices were backed by thin (3-5  $\mu$ m) polymer film.

It should be mentioned that due to the chemical fixation procedure the most dissolved sodium proves to be removed from interstitium and, to a lesser extent, from intracellular volumes restricted by cell membranes<sup>12</sup>. However, the removal of osmotic sodium during the paraffin fixation has played a positive role in this particular case. It reduced the high background signal of osmotic sodium of the extracellular fluids to highlight the tracks of bound sodium deposits.

## 3. X-RAY FLUORESCENCE MICROSCOPY

The experiments were conducted on TwinMic beamline at ELETTRA synchrotron (Italy). The X-ray fluorescence (XRF) microanalysis of the heart tissues was provided with the help of the X-ray microscope that was developed as a multi-mode instrument for high spatial resolution spectromicroscopy at low energy X-rays. In this particular experiments, the X-ray fluorescent microscopy was combined with scanning X-ray absorption microscopy (SXRМ)<sup>13-15</sup>, while the synchrotron ring operated with the electron energy of 2.4 GeV and the current of 160 mA.

For sodium mapping the TwinMic microscope was operated in scanning mode. A pinhole of 75  $\mu$ m diameter was served as a secondary X-ray source, with the focal spot of 1.2  $\mu$ m being produced by a zone plate. The micron-scale size of the probing X-ray spot was chosen as a compromise between the spatial resolution, duration of the scan run and dimensions of regions of interest (ROI).

The incident X-ray photon energy was chosen to be 1.472 keV to ensure the best excitation and detection of the  $K_\alpha$  lines of sodium atoms ( $E = 1.041$  keV). The X-ray flux through the pinhole was about  $3 \cdot 10^9$  photons/s that enabled to produce

---

\* The experiments were carried out in accordance with the international rules of the Guide for the Care and Use of Laboratory Animals and were approved by the Laboratory Animal Care and Use Commission and Local Ethics Committee at Pirogov Russian National Research Medical University.

a proper XRF signal on seven silicon drift detectors with an exposure time of 5 s. The measured XRF K-line signals of chemical elements were processed by using open source PyMCA software<sup>16</sup> to compose the chemical element mapping.

The absorption contrast SXR images were recorded with fast readout CCD camera (Andor Technology) to provide SXR images of cardiomyocytes and interstitial space as supplementary information to X-ray fluorescence maps.

The TwinMic configuration and experimental conditions enabled a successful visualization of the myocardial cellular structure and chemical element mapping of sodium, magnesium, oxygen, and other elements with precise overlapping of obtained morphological and chemical data. The XRF/SXR image sizes of ROIs varied from 50x50 to 72x72 pixels, i.e. from 60 x 60  $\mu\text{m}^2$  to 86.4 x 86.4  $\mu\text{m}^2$ . All 19 ROIs selected on 7 samples (3 ROIs per sample on all the samples except two) of myocardial tissues have been studied with using both XRF and SXR microscopy modes (see Table 1).

Table 1. Sodium XRF maps (top row) and absorption contrast X-ray images (bottom row) of different regions of interest (ROI) of myocardia slices taken from rats of two groups: samples K5 and K7 are heart tissues of normal (control) diet group, samples B1-B4, B7 are heart tissues of high sodium diet group. The ROI dimensions are defined as (60..86.4) x (60...86.4)  $\mu\text{m}^2$ .

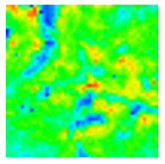
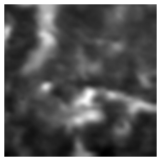
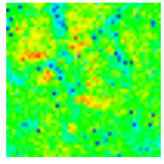
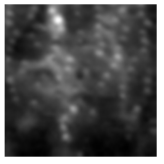
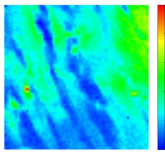
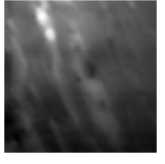
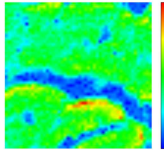
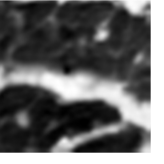
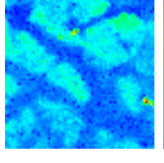
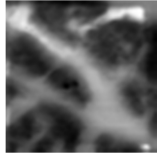
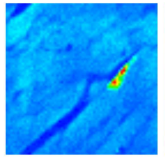
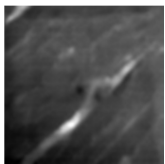
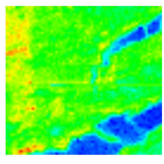
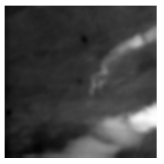
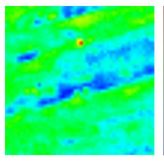
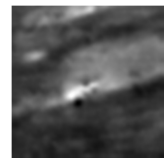
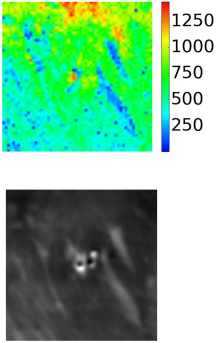
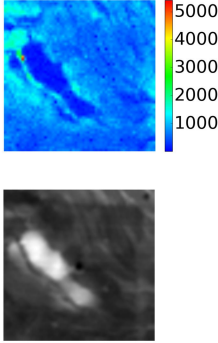
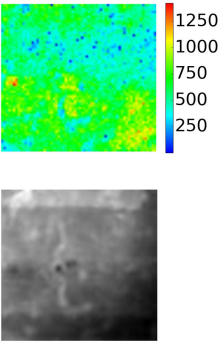
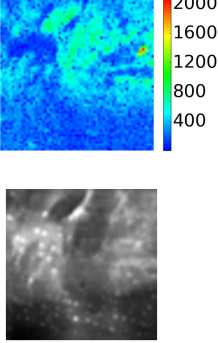
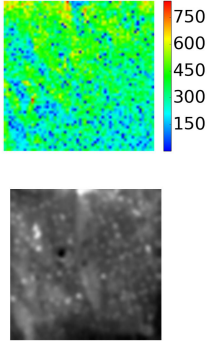
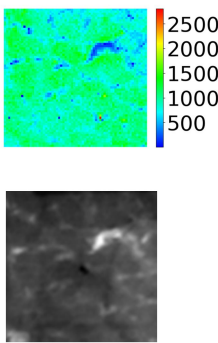
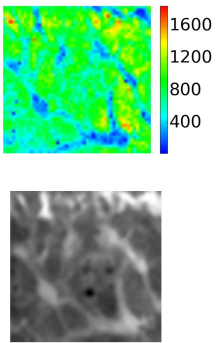
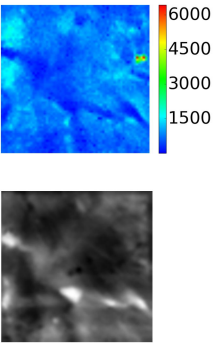
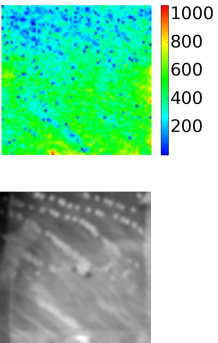
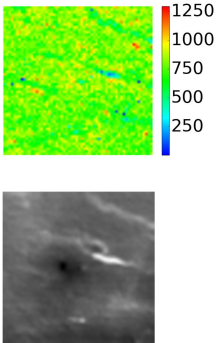
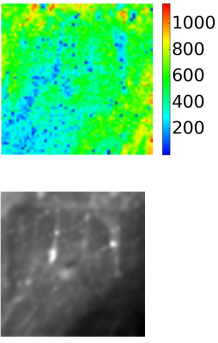
	ROI # 1	ROI # 2	ROI # 3
Sample K5	 	 	N/A
Sample K7	 	 	 
Sample B1	 	 	 

Table 1. Continuation.

Sample B2			
Sample B3			N/A
Sample B4			
Sample B7			

Thus, Table 1 shows a set of X-ray absorption images and corresponding sodium maps acquired with the help of synchrotron based STXM and XRF microscopy for heart tissue slices of high and low sodium diet animals: 5 samples were extracted from 5 rats of high sodium diet group and 2 samples were taken from 2 rats of the control group. The obtained STXM and XRF microscopy images enabled a clear visual segmentation of cardiomyocytes and intercellular spaces in the heart muscle tissues. In all samples the XRF analysis revealed a higher concentration of the sodium content inside the cells than in the interstitium space. This inverted ratio between intracellular and extracellular sodium concentrations can be explained by a strong wiping out of light metals during the chemical fixation procedure (see Section 2).

The main challenge in the statistical processing was to perform an accurate data sampling inside and outside boundaries of cardiomyocytes in the context of thin slice 3D-to-2D transformation of muscle fibers and possible interstitium perforation. This problem has been solved by using the SXR images for careful manual sampling of six 3x3 pixels ( $3.6 \times 3.6 \mu\text{m}^2$ ) zones inside every ROI to present 3 values of intracellular and 3 values of extracellular sodium content. The sampling generated the dataset of local sodium K-line emission values that could be used for the calculation of averaged intracellular and extracellular values in the ROI. The detailed description of our statistical processing of the data is beyond the scope of this paper and will be published later<sup>17</sup>.

Preliminary estimation of the relative sodium concentration results in a statistically significant difference of the sodium content in interstitium outside cardiomyocytes:  $718.0 \pm 402.4$  for high sodium diet in comparison of  $496.6 \pm 283.5$  for low sodium diet, i.e it demonstrates an elevated level in the heart tissues of high sodium diet animals. Note that we did not measure the real values of sodium concentration in the tissues because our interest was focused at study relative change of sodium content affected by the sodium diet type. We have to mention also poor statistics of the experiments due to the small number of the sampling points and samples that made us use complicated methods for statistical analysis, such as Kruskal-Wallis and Mann-Whitney tests.

To sum-up, we were able to present an experimental demonstration of elevated sodium content inside interstitium of myocardia of high sodium diet animals as compared to animals of the control group with low sodium diet. The obtained elevation of the sodium concentration cannot be explained in the frames of the normal balance of osmotic sodium in interstitium fluids and is considered to be the results of sodium depositions.

#### 4. CONCLUSIONS

To our knowledge, this paper presents the world's first high resolution X-ray imaging of myocardial cells by means of transmission and fluorescence X-ray microscopy techniques. The results show a statistically relevant increase of sodium content in interstitium of myocardia that can be explained by the new concept of sodium depositing and confirm the original assumption on the existence of osmotically inactive sodium allegedly bound with negatively charged glycosaminoglycans inside the interstitium network.

We consider this work as a beginning of new research of previously unknown structures and their effects on heart function. The next step will be a new series of similar X-ray experiments to improve the statistical properties of the sampling and a combined study of sodium and GAG structures by using XRF and FTIR-spectromicroscopy methods to validate glycosaminoglycan-sodium relation.

The authors thank Dr. N.L.Popov (LPI RAS) for his help and useful comments regarding the study and manuscript. This work was supported by CALIPSOplus EU network travel grant (20185066). The FISR Project "Tecnopolo di nanotecnologia e fotonica per la medicina di precisione" (funded by MIUR/CNR, CUP B83B17000010001) and the TECNOMED project (funded by Regione Puglia, CUP B84I18000540002) are acknowledged for financial support as well. The research leading to this result has been supported by the project CALIPSOplus under Grant Agreement 730872 from the EU Framework Programme for Research and Innovation HORIZON 2020.

## REFERENCES

- [1] Laffer, C. L., Scott III, R. C., Titze, J. M., Luft, F. C. and Elijovich, F., “Hemodynamics and salt-and-water balance link sodium storage and vascular dysfunction in salt-sensitive subjects,” *Hypertension*, 68(1), 195-203 (2016)..
- [2] Johnson, R. S., Titze, J. and Weller, R., “Cutaneous control of blood pressure,” *Current Opinion in Nephrology and Hypertension*, 25(1), 11 (2016).
- [3] Titze, J., Shakibaei, M., Schafflhuber, M., Schulze-Tanzil, G., Porst, M., Schwind, K. H., Dietsch, P. and Hilgers, K. F., “Glycosaminoglycan polymerization may enable osmotically inactive Na<sup>+</sup> storage in the skin,” *American Journal of Physiology-Heart and Circulatory Physiology*, 287(1), H203-H208 (2004).
- [4] Titze, J., Lang, R., Ilies, C., Schwind, K. H., Kirsch, K. A., Dietsch, P., Luft, F. C. and Hilgers, K. F., “Osmotically inactive skin Na<sup>+</sup> storage in rats,” *American Journal of Physiology-Renal Physiology*, 285(6), F1108-F1117 (2003).
- [5] Rakova, N., Jüttner, K., Dahlmann, A., Schröder, A., Linz, P., Kopp, C., Rauh, M., Goller, U., Beck, L. and Agureev, A., “Long-term space flight simulation reveals infradian rhythmicity in human Na<sup>+</sup> balance,” *Cell Metabolism*, 17(1), 125-131 (2013)..
- [6] Hammon, M., Grossmann, S., Linz, P., Kopp, C., Dahlmann, A., Garlichs, C., Janka, R., Cavallaro, A., Luft, F. C. and Uder, M., “<sup>23</sup>Na Magnetic Resonance Imaging of the Lower Leg of Acute Heart Failure Patients during Diuretic Treatment,” *PLoS One*, 10(10), e0141336 (2015).
- [7] Christa, M., Weng, A. M., Geier, B., Wörmann, C., Scheffler, A., Lehmann, L., Oberberger, J., Kraus, B. J., Hahner, S. and Störk, S., “Increased myocardial sodium signal intensity in Conn’s syndrome detected by <sup>23</sup>Na magnetic resonance imaging,” *European Heart Journal-Cardiovascular Imaging*, 20(3), 263-270 (2019).
- [8] Arutyunov, G., Dragunov, D., Sokolova, A., Papyshov, I., Kildyushov, E., Negrebetsky, V. and Fedorova, V., “The effect of the level of total sodium deposited in the myocardium on its stiffness,” *Therapeutic Archive*, 89(1), 32-37 (2017) (in Russian).
- [9] Kwon, T.-H., Nielsen, J., Masilamani, S., Hager, H., Knepper, M. A., Frøkiær, J. and Nielsen, S., “Regulation of collecting duct AQP3 expression: response to mineralocorticoid,” *American Journal of Physiology-Renal Physiology*, 283(6), F1403-F1421 (2002).
- [10] Kim, G.-H., Masilamani, S., Turner, R., Mitchell, C., Wade, J. B. and Knepper, M. A., “The thiazide-sensitive Na–Cl cotransporter is an aldosterone-induced protein,” *Proceedings of the National Academy of Sciences*, 95(24), 14552-14557 (1998)..
- [11] Patten, R. D. and Hall-Porter, M. R., “Small animal models of heart failure: development of novel therapies, past and present,” *Circulation: Heart Failure*, 2(2), 138-144 (2009).
- [12] Chwiej, J., Szczerbowska-Boruchowska, M., Lankosz, M., Wojcik, S., Falkenberg, G., Stegowski, Z. and Setkiewicz, Z., “Preparation of tissue samples for X-ray fluorescence microscopy,” *Spectrochimica Acta Part B: Atomic Spectroscopy*, 60(12), 1531-1537 (2005).
- [13] Gianoncelli, A., Kourousias, G., Merolle, L., Altissimo, M. and Bianco, A., “Current status of the TwinMic beamline at Elettra: a soft X-ray transmission and emission microscopy station,” *Journal of Synchrotron Radiation*, 23(6), 1526-1537 (2016).
- [14] Gianoncelli, A., Morrison, G., Kaulich, B., Bacescu, D. and Kovac, J., “Scanning transmission x-ray microscopy with a configurable detector,” *Applied Physics Letters*, 89(25), 251117 (2006).
- [15] Gianoncelli, A., Kaulich, B., Alberti, R., Klatka, T., Longoni, A., De Marco, A., Marcello, A. and Kiskinova, M., “Simultaneous soft X-ray transmission and emission microscopy,” *Nuclear Instruments and Methods in Physics Research Section A: Accelerators, Spectrometers, Detectors and Associated Equipment*, 608(1), 195-198 (2009).
- [16] Solé, V., Papillon, E., Cotte, M., Walter, P. and Susini, J., “A multiplatform code for the analysis of energy-dispersive X-ray fluorescence spectra,” *Spectrochimica Acta Part B: Atomic Spectroscopy*, 62(1), 63-68 (2007).
- [17] Artyukov, I., Arutyunov, G., Bobrov, M., Bukreeva, I., Cedola, A., Dragunov, D., Feshchenko, R., Fratini, M., Gianoncelli, A., Mitrokhin, V., Sokolova, A., Vinogradov, A., “The first observation of osmotically neutral sodium accumulation in myocardial interstitium”, *Scientific Reports* (2021) (to be published).